Single-Phase BLDC Motors for External Fan Applications

John Emmanuel Tan, Juan Paolo Quismundo, Mark Angelo Tarvina | Power Integrations, Philippines

Abstract

In order to improve efficiency across a range of applications, brushless direct current (BLDC) motors are being used to replace induction motors. This paper explores the feasibility of utilizing a single-phase BLDC motor for external fan applications with respect to operation incident external airflow and in mitigating their increased torque ripple. A method for improving alignment to support different startup conditions is also described. Compensation for increased torque ripple is addressed by both changing motor construction and control methods. Finally, a Hall-based imbalance handling algorithm is also proposed.

1. Introduction

Single-phase BLDC motors are widely used, especially in fan applications [1]. The advantages of replacing universal motors with 3-phase and single-phase BLDC motors in vacuum cleaners have been described [2]. The single-phase BLDC motor is suitable for outdoor fans where noise requirements are less stringent. Replacing the 3-phase motor with a single-phase design allows simplification of motor construction, as well as control and inverter requirements.

Single-phase motors are driven by the full-bridge inverter shown in Fig. 1(b), which uses fewer power switches and drive components than the 3-phase inverter shown in Fig. 1(a).

Hall effect sensors are widely used for determining rotor position, but sensorless control methods have now also been developed. With a sensorless approach, phase current information is used to determine proper commutation timing [3].

2. Startup Conditions

Applications with external fans, such as the air conditioning units shown in Fig. 2, require special handling due to the incidence of external air flow (wind) that can affect startup.

2.1 External Wind Conditions

The fan may startup with no wind as shown in Fig. 3(a). The external wind may also blow into the fan, driving the fan blade to rotate opposite to the desired direction. This condition, shown in Fig. 3(b), is called the headwind condition. The external wind may also blow through the back of the fan, driving the fan blade to rotate in the desired direction. This condition, shown in Fig. 3(c), is referred to as the tailwind condition.

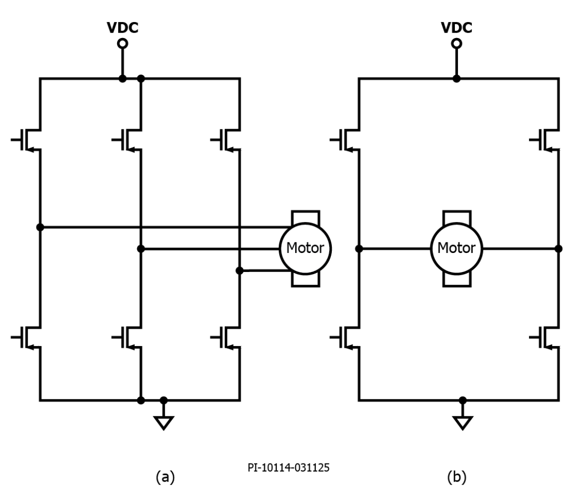

Fig. 1 Inverter for BLDC motors: (a) 3-phase, (b) single-phase

The headwind and tailwind conditions need to be considered as they affect startup and load for the single-phase fan. This is described in Section 5.

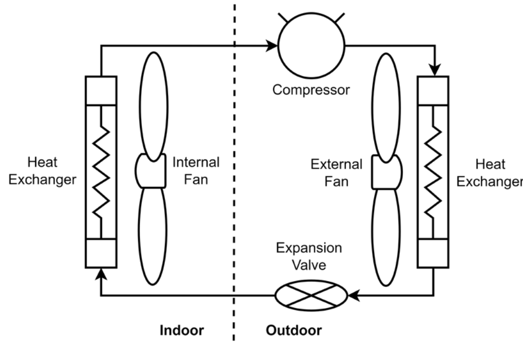

Fig. 2 Air conditioning system with external fan

2.2 Sensorless Control With Improved Alignment and Startup

A ramping voltage applied for a long duration improves the alignment of the motor [3]. This approach reduces fan blade oscillation typically caused when a constant voltage is applied during the alignment phase.

For startup and closed-loop operation, phase current information can be used for fully-sensorless operation using the current observer method [4].

3. Torque Ripple

Single-phase BLDC motors inherently have higher torque ripple compared to their 3-phase counterparts. The cogging torque profile is influenced by the motor's construction [5]. The higher torque ripple is produced by the reluctance torque produced by the interaction between the rotor permanent magnets and the ferromagnetic materials in the stator.

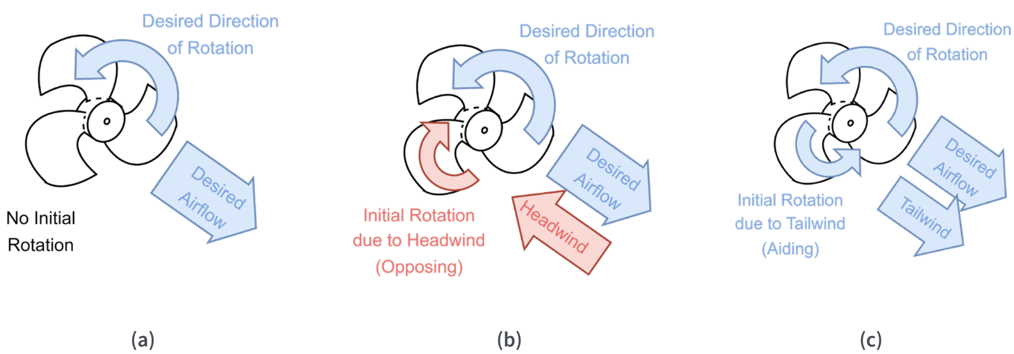

Fig. 3 Initial startup conditions: (a) no wind, (b) headwind, and (c) tailwind

A common method to improve single-phase motor cogging and starting torque is to use an asymmetric air gap [5] which also sets the preferred direction of rotation.

3.1 Cogging Torque Measurement

The cogging torque profile of the motor can be measured using a torque sensor. However, a much simpler method to measure the cogging torque is available [6].

The method employs a balanced beam acting as a lever arm that pushes down on a digital weighing scale, as shown in Fig. 4. A preload weight ensures that both positive and negative cogging torque is measured.

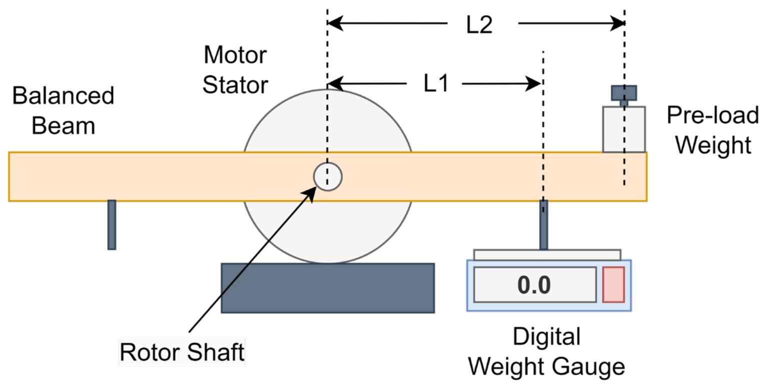

Fig. 4 Indirect cogging torque measurement

The cogging torque profile can be used to select the most appropriate driving method for torque ripple reduction.

4. Drive Methods

As described above, single-phase motors are driven by full-bridge inverters as shown in Fig. 1(b). Different drive techniques can be used to reduce the operating torque ripple for single-phase motors [7] and rotor position information is usually provided by Hall sensors.

4.1 Sensored Square Wave Drive

A typical square wave drive for single-phase motors works by applying a positive voltage across the stator winding when the Hall sensor state is high. When the Hall sensor state is low, a negative voltage is applied to the stator winding. The sensored square wave drive is shown in Fig. 5.

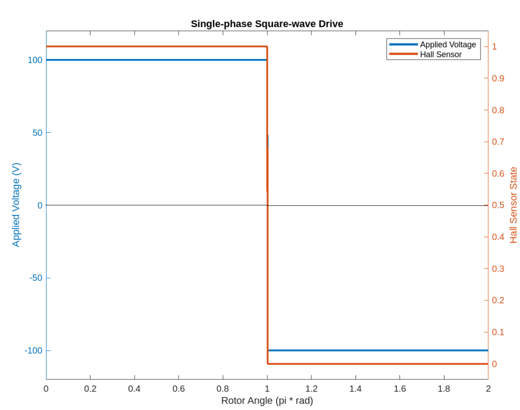

Fig. 5 Sensored square wave drive based on Hall sensor state

4.2 Sensored Current Shaping Drive

The shape of the applied voltage can be modulated to change the shape of the current. This alters the torque produced by the motor [7].

This is created by modulating either the high-side or low-side pulse width modulation (PWM) signals used to drive the full-bridge inverter switches.

Figure 6 shows an example of a sinusoidally modulated drive. The applied voltage waveshape can be adjusted to improve the operating parameters such as efficiency or torque ripple.

4.3 Sensored Drive With Commutation Pulse Control

The typical square wave drive shown in Section 4.1 will not work for high-speed fans due to high current peaks. The commutation pulse control method is developed to support this use case [8].

Dead time is added to the applied voltage at the start and/or the end of the Hall-state period. Figure 7 shows a possible configuration where the dead time (0 V applied) is inserted at both the start and the end of the Hall-state periods.

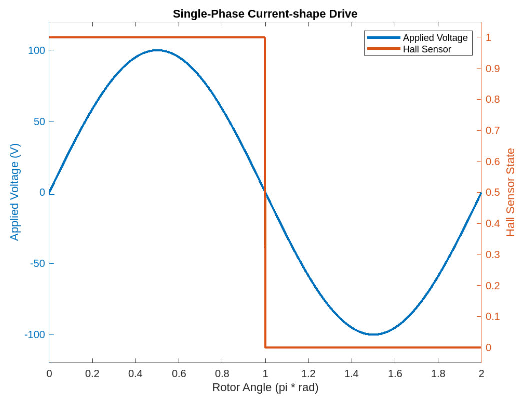

Fig. 6 Sensored current-shaping (sinusoidal) drive based on Hall sensor state

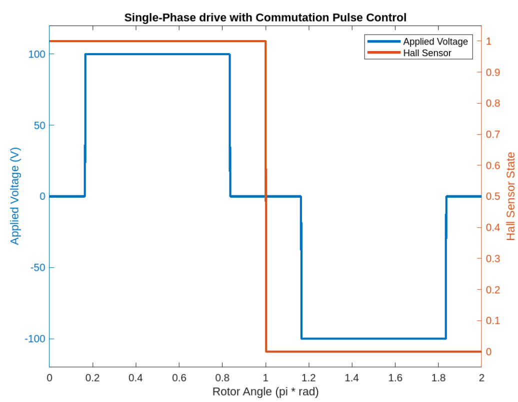

Fig. 7 Sensored square wave drive with commutation pulse control on Hall sensor state

Note that this technique is compatible with the current shaping described in Section 4.2. The applied voltage with dead time inserted can be modulated.

4.4 Sensored Hall-Imbalance Handling

The Hall sensor output may also present problems. An example is shown in Fig. 8(a), where the back-EMF (purple) is compared to the Hall sensor output (blue).

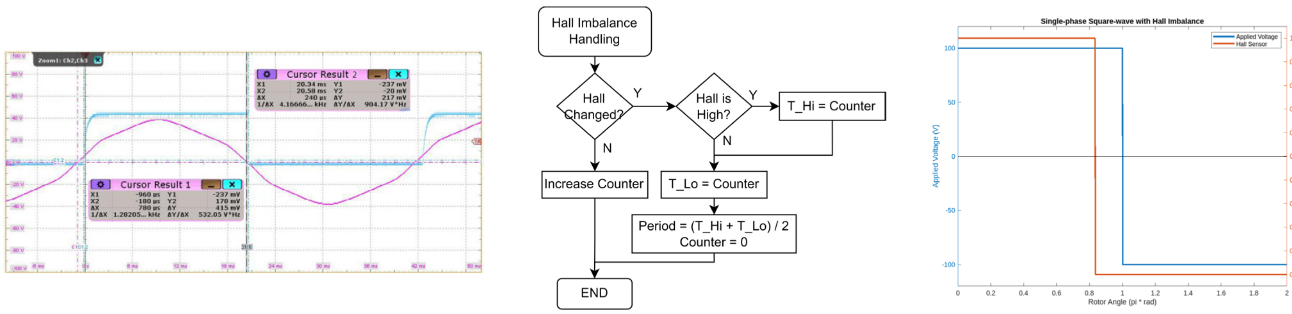

(a) (b) (c)

Fig. 8 Hall sensor imbalance: (a) motor back-EMF and Hall sensor, (b) proposed Hall-imbalance control algorithm, and (c) proposed Hall-imbalance drive technique

Hall sensor output is normally high when the back-EMF voltage is greater than 0 V. In Fig. 8(a), there is a significant delay between the Hall sensor output going high (Cursor Result 1: 700 ųs) compared to when the Hall sensor output goes low (Cursor Result 2: 240 ųs) because of the back-EMF voltage.

A Hall imbalance correction algorithm is proposed in Fig. 8(b). The resulting drive waveform is shown in Fig. 8(c). Note that the positive and negative applied voltage (blue) is balanced even when the high and low Hall sensor output states are imbalanced.

4.5 Sensorless Control

A fully-sensorless drive solution using motor phase current information can be performed by using the inflection point on the motor phase current [8]. The inflection points coincide with the back-EMF voltage zero-crossing.

5. Experimental Results

For this paper, we used a 10-pole single-phase BLDC motor with reference design kit RDK-872 from Power Integrations®. The inverter RDK uses 2 integrated half-bridge BridgeSwitch™ BRD1261C ICs. The Infineon® low-cost 32-bit ARM® Cortex®-M0 microcontroller, XMC1300, is used with the MotorXpert™ software suite from Power Integrations, which supports single-phase motor control.

5.1 External Wind Conditions

The 900 RPM single-phase BLDC motor can be used to drive the external fan of an air conditioning unit.

Figure 9 shows the operation with a headwind driving the fan to spin initially in the opposite (to desired) direction at 400 RPM.

Figure 9(a) shows the ramping alignment and startup in the headwind condition. Initially, the current oscillation indicates the non-zero back-EMF of the spinning motor due to the headwind. Figure 9(b) shows the subsequent closed-loop operation using the current observer method (RMS phase current at ~391 mA).

Figure 10 shows the operation with no wind. The motor is stationary before power is applied.

Figure 10(a) shows the ramping alignment and startup for the no headwind condition. Initially, there are no current oscillations since the back-EMF is zero for a static motor. Figure 10(b) shows closed-loop operation using the current observer method (RMS phase current at ~360 mA).

Note that the headwind increased the load on the single-phase motor such that the RMS phase current is around ~31 mA higher compared to the no wind condition.

(a) (b)

Fig. 9 Phase current during headwind condition: (a) alignment and startup, and (b) sensorless closed-loop operation

5.2 Measured Cogging Torque

Figure 11 shows the measured cogging torque using the indirect method discussed in Section 3. The negative cogging torque at around 180° can be improved to reduce the operating torque ripple by using a shaped air gap [5].

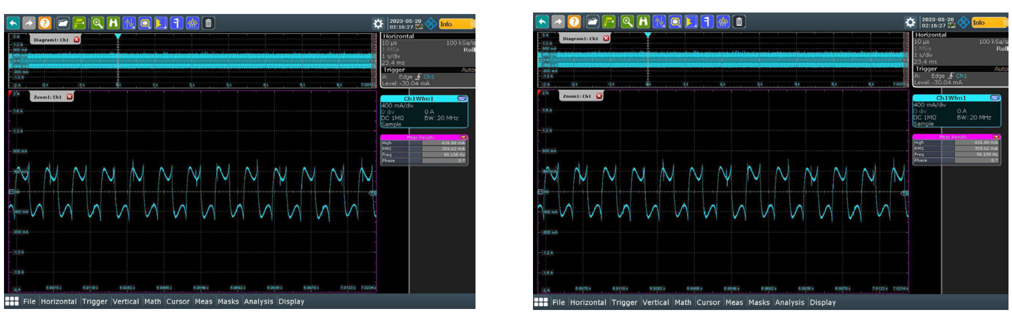

(a) (b)

Fig. 10 Phase current during no wind condition: (a) alignment and startup, and (b) sensorless closed-loop operation

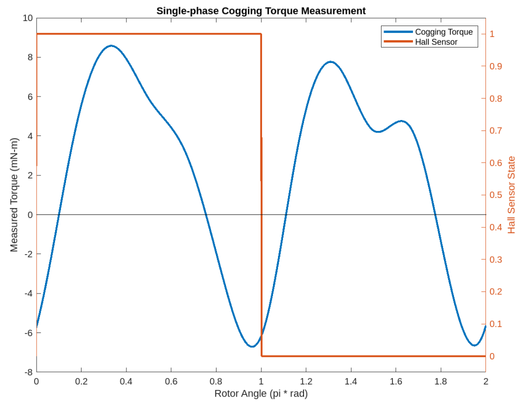

Fig. 11 Indirect cogging torque

5.3 Sensored Control

Figure 12 shows the phase current waveform when the motor runs with the sensored control methods discussed in Section 4.

For this motor, the square wave drive shown in Fig. 12(a) is only able to drive the motor up to 500 RPM, due to the very high current peaks.

Square wave drive with commutation pulse control can drive the motor up to 900 RPM as shown in Fig. 12(b). The dead time inserted is 25 percent at the end of the Hall-state period. The RMS phase current is ~350 mA.

The proposed solution for Hall imbalance handling, shown in Fig. 12(c), lowers the RMS phase current to ~316 mA.

6. Conclusion

Single-phase BLDC motors have less cost compared to 3-phase motors in terms of the motor construction and inverter components. However, the higher torque ripple produces more vibration and audible noise which limits their deployability. Applications with less stringent noise requirements, such as for external fans, are suitable for this approach.

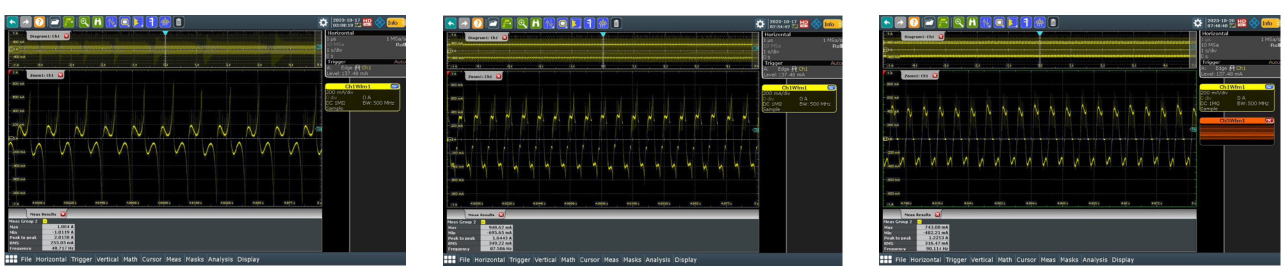

(a) (b) (c)

Fig. 12 Phase current waveform during sensored control: (a) square wave drive, (b) commutation pulse control, dead time at the ending 25 percent of the Hall-state period, and (c) proposed Hall-imbalance handling solution with dead time insertion (ending 25 percent of the Hall-state period)

For future work, a comparison between a 3-phase fan and an optimized single-phase fan can be performed using a range of performance parameters – system efficiency, inverter efficiency, and audible noise. The change in the number of components must be considered to determine if the reduction in system cost is worth the resulting performance degradation. Another avenue for research will be to explore other applications in noise-insensitive environments, such as furnace inducer fans or water pumps.

References

[1] D. Ionel, “High-efficiency variable-speed electric motor drive technologies for energy savings in the US residential sector,” in Proc. 12th Int. Conf. Optim. Electr. Electron. Equip., Brasov, Romania, May 2010.

[2] S. Bentouati, Z. Q. Zhu, and D. Howe, “Permanent magnet brushless DC motors for consumer products,” in Proc. 9th Int. Conf. Electr. Mach. Drives, Canterbury, U.K., pp. 118–122, Sep. 1999.

[3] J. E. Tan, J. M. Calderon, E. Antonio, and J. H. Puente, “Motor alignment control,” United States Patent 11,996,795, Oct. 12, 2023.

[4] J. M. Calderon, J. E. Tan, and J. H. Puente. “Sensorless control method for single-phase BLDC motors based on phase current information.” in IEEE Applied Power Electronics Conference and Exposition (APEC), pp. 1598-1601, 2022.

[5] S. Bentouati, Z. Q. Zhu, and D. Howe, “Influence of design parameters on the starting torque of a single-phase PM brushless DC motor,” in IEEE Transactions on Magnetics, vol. 36, no. 5, pp. 3533-3536, Oct. 2000.

[6] Z. Q. Zhu, “A simple method for measuring cogging torque in permanent magnet machines,” in IEEE Power & Energy Society General Meeting, pp. 1-4, Jul. 2009.

[7] L. Sun, Q. Feng, and J. Shang, “Drive of single-phase brushless DC motors based on torque analysis,” in IEEE Transactions on Magnetics, vol. 43, no. 1, pp. 46-50, Jan. 2007.

[8] Z. Q. Zhu, S. Bentouati, and D. Howe, “Control of single-phase permanent magnet brushless DC drives for high-speed applications,” in International Conference on Power Electronics and Variable Speed Drives (IEE Conf. Publ. No. 475), Sep. 2000.

For more information,
visit **power.com™**

050525